Table 1 Power indices of time decay associated with density fluctuations if $\epsilon \propto t^{-\gamma}$, $\epsilon_{\delta n} \propto t^{-\xi}$, and $k_0 r_0 \propto (\epsilon t^2/\nu)^x \propto (t^{x(2-\gamma)})$

QUANTITY	SELF PRESERVING	INERTIAL RANGE REGION ($k_0 r_0 \ll 1$)							LATE DECAY REGION ($k_0 r_0 \gg 1$)	
		GENERAL		$\langle(\delta n_e)^2\rangle \propto k_0^{3+2n}$		$r_0 \propto \epsilon^{-1/4}$	$k_0 \propto \epsilon^{1/4}$	WEBB	GENERAL	$\langle(\delta n_e)^2\rangle \propto \left(\frac{k_0}{r_0}\right)^{3/2+n}$
		$1 < \mu < 3$	$\mu > 3$	$1 < \mu < 3$	$\mu > 3$	$1 < \mu < 3$	$\mu > 3$	$\mu = \frac{5}{3}$		
$\epsilon_{\delta n}$	-4	$-\xi$	$-\xi$	$-\frac{5}{2} - n + (3+2n)(2-\gamma)(3-\mu)\frac{x}{2}$	$-\frac{5+2n}{2}$	$-\xi$	-4	$-\frac{7}{3}$	$-\xi$	$-\frac{5+2n}{2}$
ϵ	-2	$-\gamma$	$-\gamma$	$-\gamma$	$-\gamma$	$-\gamma$	-2	$-\frac{7}{3}$	$-\gamma$	$-\gamma$
$\langle(\delta n_e)^2\rangle$	-3	$1-\xi$	$1-\xi$	$-\frac{(3+2n)}{2}[1-(2-\gamma)(3-\mu)x]$	$-\frac{3+2n}{2}$	$1-\xi$	-3	$-\frac{4}{3}$	$1-\xi$	$-\frac{3+2n}{2}$
ϵt^2	const	$2-\gamma$	$2-\gamma$	$2-\gamma$	$2-\gamma$	$2-\gamma$	const	$-\frac{1}{3}$	$2-\gamma$	$2-\gamma$
k_0	$-\frac{1}{2}$	$\frac{-1+(2-\gamma)(3-\mu)x}{2}$	$-\frac{1}{2}$	$-\frac{1}{2}+(2-\gamma)(3-\mu)\frac{x}{2}$	$-\frac{1}{2}$	$\frac{-4+\gamma(3-\mu)}{4(\mu-1)}$	$-\frac{1}{2}$	$-\frac{1}{3}$	$-\frac{1}{2}+(2-\gamma)\frac{x}{2}$	$-\frac{1}{2}+(2-\gamma)\frac{x}{2}$
r_0	$\frac{1}{2}$	$\frac{1+(2-\gamma)(\mu-1)x}{2}$	$\frac{1+2x(2-\gamma)}{2}$	$\frac{1}{2}+(2-\gamma)(\mu-1)\frac{x}{2}$	$\frac{1}{2}+x(2-\gamma)$	$\frac{\gamma}{4}$	$\frac{1}{2}$	$\frac{7}{12}$	$\frac{1}{2}+(2-\gamma)\frac{x}{2}$	$\frac{1}{2}+(2-\gamma)\frac{x}{2}$
$k_0 r_0$	const	$(2-\gamma)x$	$(2-\gamma)x$	$(2-\gamma)x$	$(2-\gamma)x$	$-\frac{(2-\gamma)}{2(\mu-1)}$	const	$\frac{1}{4}$	$x(2-\gamma)$	$x(2-\gamma)$
$\lambda_{\delta n}$	$\frac{1}{2}$	$\frac{1}{2}$	$\frac{1}{2}$	$\frac{1}{2}$	$\frac{1}{2}$	$\frac{1}{2}$	$\frac{1}{2}$	$\frac{1}{2}$	$\frac{1}{2}$	$\frac{1}{2}$
$\Lambda_{\delta n}$	$\frac{1}{2}$	$\frac{1-(2-\gamma)(3-\mu)x}{2}$	$\frac{1}{2}$	$\frac{1}{2}-(2-\gamma)(3-\mu)\frac{x}{2}$	$\frac{1}{2}$	$\frac{4-\gamma(3-\mu)}{4(\mu-1)}$	$\frac{1}{2}$	$\frac{1}{3}$	$\frac{1}{2}$	$\frac{1}{2}$

two limits are shown in Table 1. The self-preserving solution arises with $\gamma = 2$, but it does not obey the Loitsianskii invariant. Another self-preserving solution that obeys the invariant (not shown in the table) is obtained by setting $x = 0$, and $\xi = (2n + 5)/2$. For $n = 0$, this corresponds to the solution given in Hinze (Ref. 3, p. 237). However, ϵt^2 is not constant in time. Other solutions are obtained by assuming the Loitsianskii invariant, viz., $\langle(\delta n_e)^2\rangle \propto k_0^{3+2n}$ for the initial stage and $\langle(\delta n_e)^2\rangle \propto (k_0/r_0)^{(3+2n)/2}$ for the final stage. Otherwise, we inspect all the various power law ranges in wave number for scalar additives postulated by various authors (see Ref. 3, pp. 232–4) and note that these can be deduced with the proportionalities that $r_0 \propto \epsilon^{-1/4}$ for $1 < \mu < 3$ and $k_0 \propto \epsilon^{1/4}$ for $\mu > 3$.

The entry in Table 1 under "WEBB" refers to his[4] considerations or those of Proudian and Feldman,[5] who show that far down an expanding wake, the integral scale length $\Lambda_{\delta n}$ varies with axial distance X as $X^{1/3}$. They also assume a direct proportionality between $\langle(\delta U)^2\rangle$ and $\langle(\delta n_e)^2\rangle$ and take $\mu = \frac{5}{3}$ (Kolmogorov's dependence). From the table in our previous note and from the present table under $r_0 \propto \epsilon^{-1/4}$, we deduce that $\xi = \lambda = \frac{7}{3}$, and then obtain the remaining results under "WEBB."

Another example is the work of Sutton.[6] He lets $\Lambda_g \propto \Lambda_{\delta n}$, that is, the same time decay for background velocity and density fluctuations as far as the integral scale length is concerned. Again using the table in our previous Note and the present table for the inertial range region satisfying the Loitsianskii invariant (with $n = 0$), we find $x = -1/(3 - \mu)$. This yields $\epsilon \propto t^{-\gamma}$, $\langle(\delta U)^2\rangle \propto t^{1-\gamma}$, $\Lambda_g \propto \Lambda_{\delta n} \propto k_0^{-1} \propto t^{(3-\gamma)/2}$, $\epsilon_{\delta n} \propto t^{(3\gamma-11)/2}$, $\langle(\delta n_e)^2\rangle \propto t^{3(\gamma-3)/2}$ and $\lambda_g \propto \lambda_{\delta n} \propto t^{1/2}$. These proportionalties are identical to those given by Sutton (with his $m = 3(3 - \gamma)/2$).

We have shown how time-dependent effects can be more naturally incorporated into a generalized spectrum function containing two scale lengths instead of a single scale length used in most of the previous approaches. Various dependences involving powers of time are deduced and compared with previous deductions, and these predictions are extended.

References

[1] Shkarofsky, I. P., "Time Variations of Generalized Spectral Functions for Velocity Turbulence," *AIAA Journal*, Vol. 8, No. 4, April 1970, pp. 803–805.

[2] Shkarofsky, I. P., "Generalized Turbulence Space-Correlation and Wave Number-Spectrum Function Pairs," *Canadian Journal of Physics*, Vol. 46, No. 19, Oct. 1, 1968, pp. 2133–2153.

[3] Hinze, J. O., *"Turbulence,"* McGraw-Hill, New York, 1959, Chap. 3.

[4] Webb, W. H., "Self-Preserving Fluctuations and Scales for the Hypersonic Turbulent Wake," *AIAA Journal*, Vol. 2, No. 11, Nov. 1964, pp. 2031–2033.

[5] Proudian, A. P. and Feldman, S., "A New Model for Mixing and Fluctuations in a Turbulent Wake," *AIAA Journal*, Vol. 3, No. 4, April 1965, pp. 602–609, Appendix.

[6] Sutton, G. W., "Decay of Passive Scalar Fluctuations in Isotropic Homogeneous Turbulence," *The Physics of Fluids*, Vol. 11, No. 3, March 1968, p. 671.

Twisted Beam Element Matrices for Bending

Kent L. Lawrence*
University of Texas at Arlington, Arlington, Texas

In this Note, the approximate theory of bending is employed to determine the element flexibility and stiffness matrices for a uniform beam element with linear geometric

Received December 1, 1969. The author gratefully acknowledges the helpful comments of the reviewers.

* Associate Professor, Department of Engineering Mechanics. Member AIAA.

twist. Numerical data are presented to show the difference in deflections calculated using this continuous theory and those calculated by use of a number of straight uniform beam elements which are piecewise twisted.

It is assumed that the beam has a natural twist about the centroidal axis which varies linearly with the axial coordinate x. That is, $\alpha(x) = (\alpha_0/L)x$ as shown in Fig. 1. At $x = 0$, the y and z axes are aligned with the cross-section principal axes whose bending stiffnesses EI_1 and EI_2 are independent of x.

The equations governing displacements due to end loadings F_i are given by Houbolt and Brooks[1]

$$(EI_1 \cos^2\beta x + EI_2 \sin^2\beta x)w'' + (EI_2 - EI_1)\sin\beta x \cos\beta x v'' = My = F_2(L - x) - F_3 \quad (1)$$

$$(EI_1 - EI_2)\sin\beta x \cos\beta x w'' + (EI_1 \sin^2\beta x + EI_2 \cos^2\beta x)v'' = Mz = F_1(L - x) + F_4 \quad (2)$$

where $\beta = \alpha_0/L$ and primes denote derivatives with respect to x. The moment Mz is taken according to the right-hand rule, while My is in accord with the left-hand rule. Introducing the double angle $\gamma = 2\beta$ and using the notation $Q = (EI_2 + EI_1)/2$, $R = (EI_2 - EI_1)/2$, and $D = 1/(Q^2 - R^2)$, Eqs. (1) and (2) may be separated and integrated to give the following displacement functions:

$$w'(x) = D[(F_2L - F_3)Qx + (F_2L - F_3)R(\sin\gamma x)/\gamma - F_2Qx^2/2 - F_2R(\cos\gamma x + \gamma x \sin\gamma x)/\gamma^2 + (F_1L + F_4)R(\cos\gamma x)/\gamma - (F_1L + F_4)R \times (\sin\gamma x - \gamma x \cos\gamma x)/\gamma^2] + B_1 \quad (3)$$

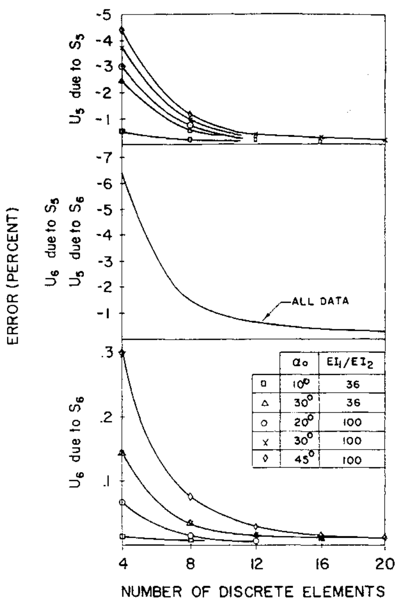

Fig. 2 Cantilever deflections.

$$v(x) = D[(F_1L + F_4)Qx^2/2 + (F_1L + F_4)R(\cos\gamma x)/\gamma^2 - F_1Qx^3/6 + F_1R(2\sin\gamma x - \gamma x\cos\gamma x)/\gamma^3 + (F_2L - F_3)R \times (\sin\gamma x)/\gamma^2 - F_2R(2\cos\gamma x + \gamma x \sin\gamma x)/\gamma^3] + B_3x + B_4 \quad (6)$$

where the B_i are constants of integration.

The flexibility matrix below is found from Eqs. (3–6) by imposing fixed boundary conditions at $x = 0$ and evaluating the displacements at $x = L$ for successive loadings $F_i = 1$.

$$[f] = D \times$$

$$\begin{array}{cc}
\begin{array}{cccc} 1 & 2 & 3 & 4 \end{array} & \\
\begin{bmatrix}
L^3[Q/3 - 2R(\Delta - \sin\Delta)/\Delta^3] & RL^3[2(1-\cos\Delta)/\Delta^3 - 1/\Delta] & RL^2[(\Delta - \sin\Delta)/\Delta^2] & L^2[Q/2 - R(1-\cos\Delta)/\Delta^2] \\
 & L^3[Q/3 + 2R(\Delta - \sin\Delta)/\Delta^3] & -L^2[Q/2 + R(1-\cos\Delta)/\Delta^2] & -RL^2[(\Delta - \sin\Delta)/\Delta^2] \\
 & & L[Q + R(\sin\Delta)/\Delta] & RL[(1-\cos\Delta)/\Delta] \\
\text{(symmetric)} & & & L[Q - R(\sin\Delta)/\Delta]
\end{bmatrix} & \begin{array}{c} 1 \\ 2 \\ 3 \\ 4 \end{array}
\end{array} \quad (7)$$

$$w(x) = D[(F_2L - F_3)Qx^2/2 - (F_2L - F_3)R(\cos\gamma x)/\gamma^2 - F_2Qx^3/6 - F_2R(2\sin\gamma x - \gamma x\cos\gamma x)/\gamma^3 + (F_1L + F_4)R \times (\sin\gamma x)/\gamma^2 + (F_1L + F_4)R(2\cos\gamma x + \gamma x \sin\gamma x)/\gamma^3] + B_1x + B_2 \quad (4)$$

$$v'(x) = D[(F_1L + F_4)Qx - (F_1L + F_4)R(\sin\gamma x)/\gamma - F_1Qx^2/2 + F_1R(\cos\gamma x + \gamma x \sin\gamma x)/\gamma^2 + (F_2L - F_3)R \times (\cos\gamma x)/\gamma + F_2R(\sin\gamma x - \gamma x\cos\gamma x)/\gamma^2] + B_3 \quad (5)$$

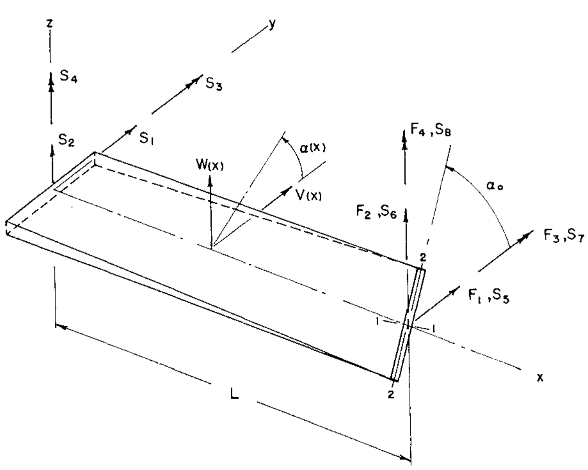

Fig. 1 Notation.

Each element of the flexibility matrix contains an indeterminate form for $\Delta = 2\alpha_0 = 0$. These, however, are reducible to the appropriate untwisted beam constants by repeated application of L'Hopital's rule.[2]

Evaluation of the element stiffness matrix from the flexibility matrix may be accomplished through use of the element equilibrium equations.[3] From Fig. 1, these may be written in terms of the element loading S_i as

$$\begin{Bmatrix} S_1 \\ S_2 \\ S_3 \\ S_4 \end{Bmatrix} + \begin{bmatrix} 1 & 0 & 0 & 0 \\ 0 & 1 & 0 & 0 \\ 0 & -L & 1 & 0 \\ L & 0 & 0 & 1 \end{bmatrix} \begin{Bmatrix} S_5 \\ S_6 \\ S_7 \\ S_8 \end{Bmatrix} = \{0\} \quad (8)$$

If the square matrix of Eq. (8) is denoted by $[T]^T$, then the stiffness matrix becomes

$$[k] = [N]^T[f]^{-1}[N] \quad (9)$$

where $[N] = [T, -I]$, $[I]$ = the identity matrix. The order of the variables in Eq. (9) is 1–8.

The utility of the element matrices of Eqs. (7) and (9) was investigated by comparing end deflections of a twisted cantilever calculated using these matrices to deflections calculated using a finite element program in which the cantilever was idealized as an assemblage of straight beam elements piecewise twisted with respect to one another. The incremental twist of each straight element was taken as the average of $\alpha(x)$ of the twisted beam over the interval modeled. Uniform element spacings were used, and the number of elements was varied from 4 to 20. The inverse of $[f]$ was evaluated numerically. The calculations were performed using a digital computer employing twelve digit accuracy for a number of EI_1, EI_2, L, and α_0 combinations. Loadings S_5 and S_6 were applied independently, and deflections $u_5 - u_8$ calculated in each instance. Solution by the formulations of Eqs. (7) and (9) gave identical results as expected. The % error between the segmentally twisted beam deflections and those calculated by the continuous twist formulation of Eqs. (7) and (9) is given in Fig. 2 for a few of the cases considered.

The range of parameters considered is felt to be of practical interest, and based upon the cases considered, it is evident that the errors due to segmental twist modeling are most significant for the coupling deflections and for bending which is predominantly in the stiffer plane. Also it is noted that these errors are strongly dependent upon the total twist and only little influenced by EI_1/EI_2 variations. For the several total beam lengths employed, the % error was found to be independent of this parameter. In all cases considered however, the error produced by the segmental approximation is less than 1% if the number of piecewise twisted elements employed is ten or greater.

References

[1] Houbolt, John C. and Brooks, George W., "Differential Equations of Motion for Combined Flapwise Bending, Chordwise Bending, and Torsion of Twisted Nonuniform Rotor Blades," TN 1346, 1958, NACA.

[2] Carnegie, William, "Static Bending of Pre-Twisted Cantilever Blading," *Proceedings of the Institution of Mechanical Engineers*, Vol. 171, 1957, pp. 873–894.

[3] Przemieniecki, J. S., *Theory of Matrix Structural Analysis*, McGraw-Hill, New York, 1968, pp. 148–150.

Flutter of Low Aspect Ratio Plates

E. H. Dowell* and C. S. Ventres†

Princeton University, Princeton, N.J.

SPRIGGS, Messiter, and Anderson[1] have recently presented an interesting and valuable explanation of the flutter behavior of a (two-dimensional) plate under in-plane tension load in the limit as the tension stiffness dominates the bending stiffness, i.e., a membrane. They develop an asymptotic analysis based on the hypothesis of a boundary layer at the plate edge and the presence of two length scales. The insight into this boundary-layer behavior was obtained by examining the natural modes of a pure membrane under aerodynamic loading, although there is more than a hint of such behavior in Dugundji's results[2] for plates with finite bending stiffness.

It is the purpose of the present Note to point out that the interpretation of the results of Spriggs et al. may be generalized to include three-dimensional plates and thus also explain the failure of infinitely long traveling wave analyses for low aspect ratio plates at high supersonic speeds and, implicitly, the success of such analyses at subsonic Mach numbers.[3–5]

The mathematical model studied by Spriggs, Messiter, and Anderson was a two-dimensional plate under tension using linear plate theory and piston theory aerodynamics. The equation of motion for such a physical system is (here we use essentially the notation of Dugundji[2,4] and Dowell[5])

$$D\frac{\partial^4 w}{\partial x^4} - N_x\frac{\partial^2 w}{\partial x^2} + \frac{\rho U^2}{M}\frac{\partial w}{\partial x} + \frac{\rho U}{M}\frac{\partial w}{\partial t} + \rho_m h\frac{\partial^2 w}{\partial t^2} = 0 \quad (1)$$

These equations can be nondimensionalized as

$$\epsilon^2\frac{\partial^4 w}{\partial \xi^4} - \frac{\partial^2 w}{\partial \xi^2} + \epsilon^2\lambda\frac{\partial w}{\partial \xi} + \left(\frac{\lambda\mu}{M}\right)^{1/2}\epsilon^2\frac{\partial w}{\partial \tau} + \epsilon^2\frac{\partial^2 w}{\partial \tau^2} = 0 \quad (2)$$

where

$$\epsilon^2 \equiv D/a^2N_x,\ \lambda \equiv \rho U^2a^3/DM,\ \mu \equiv \rho a/\rho_m h$$
$$\tau \equiv t(D/\rho_m h a^4)^{1/2},\ \xi \equiv x/a$$

Assuming

$$w(\xi,\tau) = \bar{w}(\xi)e^{ik\tau}$$

the eigenvalue problem becomes

$$\epsilon^2 d^4\bar{w}/d\xi^4 - (d^2\bar{w}/d\xi^2) + \epsilon^2\lambda(d\bar{w}/d\xi) + \epsilon^2 B\bar{w} = 0 \quad (3)$$

where

$$B \equiv [(\lambda\mu/M)^{1/2}iK - K^2]$$

Spriggs et al. introduced the following variables: $\alpha^2 \equiv \lambda\epsilon^3$ and $\gamma \equiv (\lambda\mu/M)^{1/2}\epsilon^3$ and obtained stability boundaries (where the imaginary part of the eigenvalue K becomes negative) in terms of α, γ, and ϵ. The specific mathematical techniques used lead to asymptotic expansions in ϵ, for small ϵ, allowing for two length scales, one of order 1 and one of order ϵ.

Now let us consider a more general problem, that of a three-dimensional plate under tension loads in two directions. (Actually, what follows could be generalized to include structural damping, an elastic foundation and orthotropicity, see for example Dugundji[2] as well as earlier work by Hedgepeth[6] and Houbolt.[7]) Thus,

$$D\left[\frac{\partial^4 w}{\partial x^4} + 2\frac{\partial^4 w}{\partial x^2\partial y^2} + \frac{\partial^4 w}{\partial y^4}\right] - N_x\frac{\partial^2 w}{\partial x^2} - N_y\frac{\partial^2 w}{\partial y^2} + \frac{\rho U^2}{M}\frac{\partial w}{\partial x} + \frac{\rho U}{M}\frac{\partial w}{\partial t} + \rho_m h\frac{\partial^2 w}{\partial t^2} = 0 \quad (4)$$

Nondimensionalizing,

$$\frac{\partial^4 w}{\partial \xi^4} + 2\frac{\partial^4 w}{\partial \xi^2\partial \eta^2}\left(\frac{a}{b}\right)^2 + \frac{\partial^4 w}{\partial \eta^4}\left(\frac{a}{b}\right)^4 - R_x\frac{\partial^2 w}{\partial \xi^2} - R_y\frac{\partial^2 w}{\partial \eta^2}\left(\frac{a}{b}\right)^2 + \lambda\frac{\partial w}{\partial \xi} + \left(\frac{\lambda\mu}{M}\right)^{1/2}\frac{\partial w}{\partial \tau} + \frac{\partial^2 w}{\partial \tau^2} = 0$$

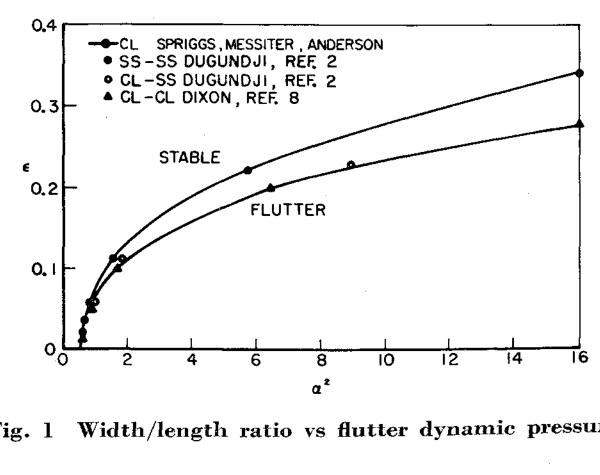

Fig. 1 Width/length ratio vs flutter dynamic pressure.

Received December 11, 1969; revision received February 13, 1970. This work was supported by NASA Grant NGR 31-001-059.

* Associate Professor, Department of Aerospace and Mechanical Sciences. Member AIAA.

† Research Associate, Department of Aerospace and Mechanical Sciences.